



# Feasibility of in vivo CAR T cells tracking using streptavidin–biotin-paired positron emission tomography

Donghui Pan<sup>1</sup> · Yan Wang<sup>2,3</sup> · Nan Xu<sup>4</sup> · Yuping Xu<sup>1</sup> · Xinyu Wang<sup>1</sup> · Lizhen Wang<sup>1</sup> · Junjie Yan<sup>1</sup> · Lei Yu<sup>4</sup> · Liyan Miao<sup>2,3</sup> · Guangji Wang<sup>5</sup> · Min Yang<sup>1</sup>

Received: 9 May 2022 / Accepted: 20 July 2022 / Published online: 29 July 2022  
© The Author(s), under exclusive licence to Springer-Verlag GmbH Germany, part of Springer Nature 2022

## Abstract

**Background** A novel reporter system, streptavidin (SA)- [<sup>68</sup>Ga]Ga-labeled biotin ([<sup>68</sup>Ga]Ga-DOTA-biotin), was constructed and its ability for PET imaging the behaviors of CAR T cells were also evaluated in this study.

**Methods** In vitro activity and cytotoxicity of the SA transduced anti-CD19-CAR T (denoted as SA-CD19-CAR T) cells were determined. The feasibility of monitoring proliferation profiles of SA-CD19-CAR T cells using [<sup>68</sup>Ga]Ga-DOTA-biotin was firstly investigated in a solid tumor model. Also, the pharmacodynamics and pharmacokinetics of the CAR T cells in whole-body hematologic neoplasms were evaluated by bioluminescence imaging and [<sup>68</sup>Ga]Ga-DOTA-biotin PET imaging simultaneously.

**Results** After transduction with SA, the activity and cytotoxicity of the modified CAR T cells were not affected. PET images revealed that the uptakes of [<sup>68</sup>Ga]Ga-DOTA-biotin in CD19<sup>+</sup> K562 solid tumors were  $0.67 \pm 0.32$  ID%/g and  $1.26 \pm 0.13$  ID%/g at 30 min and 96 h p.i. after administration of SA-CD19-CAR T cells respectively. It confirmed that the SA-CD19-CAR T cells could effectively inhibit the growth of Raji hematologic tumors. However, low radioactivity related to the proliferation of CD19-CAR T cells was detected in the Raji model.

**Conclusion** SA-CD19-CAR T cells were constructed successfully without disturbing the antitumor functions of the cells. The proliferation of the CAR T cells in solid tumors could be early detected by [<sup>68</sup>Ga]Ga-DOTA-biotin PET imaging.

**Keywords** CAR T cell · Gallium-68 · Biotin · Streptavidin · PET

## Introduction

Adoptive cell therapy (ACT) is a valid strategy for treating cancers by empowering patients' immune systems to destroy malignant cells [1, 2]. Among most ACT, chimeric antigen

receptor (CAR) T cell therapy is utilized most successfully in clinical practice [3]. Various CAR T cell therapy including Kymriah, Tecartus, and Liso-cel have been approved for treating relapsed or refractory B-cell leukemia and lymphoma [4–7].

Despite the enormous success, some challenges are encountered during the clinical translation. Different from

This article is part of the Topical Collection on Radiopharmacy.

Donghui Pan and Yan Wang contributed equally to this work.

✉ Liyan Miao  
miaolysuzhou@163.com

✉ Guangji Wang  
gjwang@cpu.edu.cn

✉ Min Yang  
yangmin@jsinm.org

<sup>1</sup> NHC Key Laboratory of Nuclear Medicine, Jiangsu Key Laboratory of Molecular Nuclear Medicine, Jiangsu Institute of Nuclear Medicine, Wuxi, Jiangsu 214063, China

<sup>2</sup> Department of Clinical Pharmacology, the First Affiliated Hospital of Soochow University, Suzhou 215006, China

<sup>3</sup> Institute for Interdisciplinary Drug Research and Translational Sciences, College of Pharmaceutical Sciences, Soochow University, Suzhou 215006, China

<sup>4</sup> School of Chemistry and Molecular Engineering, East China Normal University, Shanghai UniCAR Therapy Bio-Medicine Technology Co., Ltd, Shanghai 200062, China

<sup>5</sup> Key Laboratory of Drug Metabolism and Pharmacokinetics, State Key Laboratory of Natural Medicines, China Pharmaceutical University, Nanjing 211198, China

small molecule drugs or antibodies, the personalized CAR T cell was complex and expensive [8, 9]. Nevertheless, the in vivo dynamic behaviors of CAR T cells related to clinical efficacy such as proliferating, homing to tumor sites, and persistence were not clearly understood.

In clinical, quantitative polymerase chain reaction (qPCR) or flow cytometry is performed to analyze the functions of infused CAR T cells through the samples from peripheral blood or bone marrow [10, 11]. However, the outcomes cannot accurately predict the efficacy due to the influence of factors such as tumor burdens, heterogeneity, and individual difference [12, 13]. Moreover, the invasive procedure might cause complications including allergy, pain, or infection, and it is difficult to be performed in real-time and multiple times. Thus, a novel precise strategy for in vivo tracking the CAR T cell and evaluating its antitumor effects was needed.

Positron emission tomography (PET) imaging is a non-invasive imaging modality to reveal the biological processes at the molecular and cellular levels in the living systems [14, 15]. It can character and visualize the dynamic biochemical changes that occurred in the body with the advantages of high sensitivity and quantity [16]. Labeling CAR T cells with radionuclides such as [ $^{89}\text{Zr}$ ]Zr-oxine is a valid imaging platform to determine the distribution of cells after adoptive transfer. However, higher radioactivity may disturb the viability and function of the cells. Meanwhile, the radio signals may be gradually diluted by the proliferation of the cells and difficult to detect [17].

Recently, reporter genes technology provides a potent strategy to track CAR T cells in vivo and evaluate their efficacy. For example, CAR T cells expressed Herpes simplex virus type 1 thymidine kinase (HSV1) have been monitored by [ $^{18}\text{F}$ ]-FHBG PET imaging in recurrent glioma [18]. Nevertheless, the reporter system may lead to immunogenicity and fail therapy. Besides, prostatic specific membrane antigen (PSMA) or somatostatin receptor 2 (SSTR2) was reported to be introduced into the CAR T cells respectively, and the behaviors of the engineered CAR T cells in mice were visualized by specific probes, [ $^{18}\text{F}$ ]-DCFPyL or [ $^{68}\text{Ga}$ ]Ga-DOTA-TOC, respectively [19, 20]. However, the receptors are also expressed in normal organs and abundant in solid tumors, which may enhance the non-specific signals and affect the image quality.

Streptavidin (SA) is a tetrameric protein purified from the bacterium streptomyces avidin. It could not be detected in normal tissue [21]. Previously, our group developed SA transduced CAR T cells (denoted as SA-CD19-CAR T cells) and its specific PET probe [ $^{68}\text{Ga}$ ]Ga-DOTA-biotin. In vitro radio-TLC measurement and in vivo PET imaging after stereotactic injection revealed that the streptavidin–biotin pair system owned favorable sensitivity and specificity [22]. In this study, the effects of SA on the functions of CD19-CAR T cells were determined through in vitro experiments and

the feasibility of monitoring the biological behaviors of the CAR T cells using [ $^{68}\text{Ga}$ ]Ga-DOTA-biotin PET imaging was evaluated in animal models. Meanwhile, the association between pharmacodynamics and pharmacokinetics of CAR T cells was also investigated.

## Materials and methods

### General

[ $^{68}\text{Ga}$ ]Ga-DOTA-biotin was synthesized according to our previous literature and the radiochemical purity was greater than 95% [22]. Other reagents were commercial and analytical grade.

### Cells

SA-CD19-CAR T cells, CD19-CAR T cells, and naive T cells were gifted from Shanghai UniCAR Therapy Biomedicine Technology Co., Ltd. The transduction efficiency of SA-CD19-CAR T cells was 12.2%. Human myelogenous leukemia cell line (wild-type K562 and CD19-positive K562) and CD19-expressing Burkitt human B lymphoma cell line (Raji and luciferase-expressing Raji cells, Raji-Luc) were also gifted from Shanghai UniCAR Therapy Biomedicine Technology Co., Ltd.

### Functional validation of SA-CD19-CAR T cells

#### Viability of CAR T cells

After transduction, the cells were cultured and expanded in a 5% CO<sub>2</sub> atmosphere at 37 °C using an AIM-V medium supplemented with recombinant human interleukin-2 and 10% fetal bovine serum. The numbers of CAR T cells were measured by Trypan Blue staining.

#### Assay for antigen-stimulated T cells proliferation

According to the manufacturer's protocol, antigen-stimulated cell proliferation assays were performed using a carboxy fluorescein diacetate succinimidyl ester (CFSE) assay kit (Selleck Chemicals). Briefly, At 96 well plates, transduced T cells (CD19-CAR T or SA-CD19-CAR T cells) and naive T cells (NC) were co-cultured for 5 days with K562 or CD19<sup>+</sup>K562 tumor cells pretreated by mitomycin (10 μg/mL) to stop division respectively. Changes in CFSE intensity were detected by flow cytometry. Data are analyzed using FlowJo V10 software (TreeStar, San Carlos, CA, USA).

### In vitro cytotoxicity assay

The cytotoxicity of anti-CD19 CAR T cells was monitored using Raji tumor cells. A number of  $2 \times 10^5$  Raji tumor cells were co-incubated with effector T cells (CAR T or NC T cells) for 6 h at 5% CO<sub>2</sub> and 37°C. The effector to target cells (E:T) ratios were from 2.5 to 10 and the total volumes were 100 µL. At selected time points, 50 µL cell-free supernatant per well was transferred to a new 96-well plate and mixed with an equal volume of lactate dehydrogenase (LDH) substrate mixture (Promega Corporation) for 30 min at room temperature in the dark. The absorbent signals of the solution at 492 nm were detected using a reader (Multiskan GO, Thermo Scientific) and the resulting dissolution rate was calculated through normalization.

### Antigen-stimulated cytokine release analysis

Cytokine release was assessed using the Th1/Th2 Cytometric Bead Array (CBA) Kit II (BD Bioscience) according to the manufacturer's instructions. Briefly, CAR T cells were co-cultured with K562 or CD19<sup>+</sup>K562 tumor cells in RPMI 1640 medium with an E:T ratio of 5:1 in 96-well plates. After incubating for 24 h, microspheres of seven specific cytokines (IL-2, IL-4, IL-6, IL-10, IFN-γ, TNF-α, and IL-17A) were added and incubated with fluorescent antibodies in cell free supernatants for 3 h. After washing, the cytokine concentrations were determined by flow cytometry and calculated from the standard curves respectively.

### Animal models

Animal experiments were approved by the ethics committee and performed under the regulations of national laws. NCG mice were purchased from GemPharmatech Co., Ltd and injected subcutaneously with CD19<sup>+</sup> K562 human myelogenous leukemia cells at the right behind flank regions. When the tumor volumes reached 100–200 mm<sup>3</sup>, the mice were used for the following experiments.

NCG mice-bearing luminescent CD19<sup>+</sup> Raji (Raji-Luc) human B lymphoma were obtained by intravenous injection of the Raji-Luc tumor cells according to the literature [23, 24]. At 3 days after administration, the model was obtained since the tumors were visualized in the mice through bioluminescence imaging.

### [<sup>68</sup>Ga]Ga-DOTA-biotin PET imaging in a solid tumor model

Mice-bearing CD19<sup>+</sup>K562 tumors were intravenously injected with  $5 \times 10^6$  CD19-CAR T cells or SA-CD19-CAR T cells ( $n = 3$  for each group). At 30 min and 96 h after introducing the cells, mice were injected with 3.7 MBq of [<sup>68</sup>Ga]

Ga-DOTA-biotin under isoflurane anesthesia respectively. Static PET scans were performed using an Inveon MicroPET scanner (Siemens Medical Solutions) at 1 h after [<sup>68</sup>Ga] Ga-DOTA-biotin administration respectively. Quantification analysis of PET images was performed using the reported method [22].

### Pharmacodynamics and pharmacokinetics study in whole body hematologic neoplasms

According to previous studies [25–28], mice-bearing Raji-Luc tumors were treated by intravenous injection of CD19-CAR T cells, SA-CD19-CAR T cells ( $5 \times 10^6$  cells), or medium ( $n = 5$  for each group) respectively. The detailed scheme was listed in Fig. 3A. Optical imaging with PerkinElmer's IVIS optical imaging systems was used to monitor the tumor burdens at 0, 3, 6, 9, 15, 21, 27, 34 days after treatment with CAR T cells or medium respectively using the reported method [29]. Furthermore, [<sup>68</sup>Ga]Ga-DOTA-biotin PET imaging was performed to assess the pharmacokinetics of CAR T cells at 0, 4, 7, 14 days after treatment with CAR T cells or medium respectively using the above PET imaging procedures.

### Statistical analysis

GraphPad Prism software was used for statistical analyses. Data were analyzed using the unpaired, 2-tailed Student *t*-test. Differences at the 95% confidence level ( $p < 0.05$ ) were considered to be statistically significant.

## Results

### Functional validation of SA-CD19-CAR T cells

#### Viability of CAR T cells

Under the same culture conditions, the numbers of CAR T cells, and naive T cells expanded with a similar trend over time. After being cultured for 10 days, the expansion folds of CAR T cells and naive T cells were greater than 100 (Fig. 1A). It also noted that the corresponding value of SA-CD19-CAR T cells was over 200 at the same time points.

#### Assay for antigen-stimulated T cells proliferation

To further confirm that transducing SA into CAR T cells does not have a negative impact on effect functions, antigen-specific proliferation assay was performed. As shown in Fig. 1B, proliferation peaks occurred after co-incubation with CD19<sup>+</sup> K562 tumor cells by SA-CD19-CAR T cells and CD19-CAR T cells respectively. Whereas, the corresponding

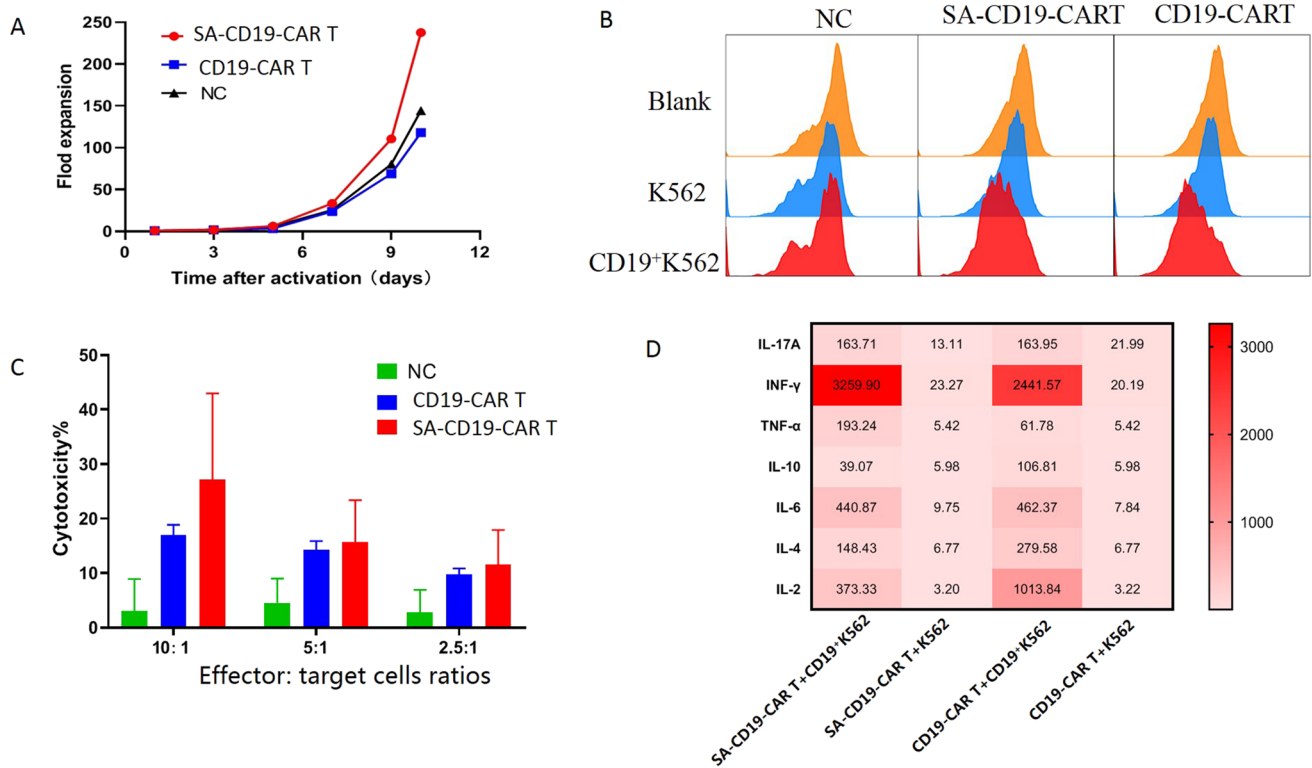


**Fig. 1** In vitro biological performance of SA-CD19-CAR T cells and CD19-CAR T cells. **A** Viability of SA-CD19-CAR T cells, CD19-CAR T cells, and T cells. **B** Results of antigen-specific proliferation ability of different CAR T cells. The orange peak indicates that effect cells were cultured separately. The blue peak indicates that effect

cells were co-cultured with K562 tumor cells. The red peak indicates that effect cells were co-cultured with CD19<sup>+</sup> K562 tumor cells. **C** Killing effect of CAR T cells on different effector: target cells ratios. **D** Heat map of antigen-stimulated cytokine release analysis

peak was not observed after co-incubation of the CD19<sup>+</sup> K562 cells with naive T cells.

#### In vitro cytotoxicity assay

Compared with the NC group, CD19-CAR T cells and SA-CD19-CAR T cells own more strong killing effects on Raji tumor cells (Fig. 1C). When the effector:target cells ratios increased from 2.5 to 10, the percentages of cytotoxicity in NC groups were  $2.77 \pm 4.16$  and  $3.02 \pm 5.90$ . In contrast, the corresponding values of CD19-CAR T cells and SA-CD19-CAR T cells changed from  $9.74 \pm 1.11$  and  $11.56 \pm 6.36$  to  $17.00 \pm 1.84$  and  $27.14 \pm 15.82$  respectively. It implied that transducing SA into CAR T cells did not affect the cytotoxicity of the cells against tumors.

#### Antigen-stimulated cytokine release analysis

After being stimulated by antigen, T cells will be activated and release cytokine to attack the tumors. As shown in Fig. 1D, the levels of cytokines released from both SA-CD19-CAR T cells and CD-19 CAR T cells after incubation with CD19<sup>+</sup>K562 tumor cells increased 10 to 100

times than those of corresponding values in wild types K562 tumor cells respectively.

In summary, in vitro experiments proved that no significant differences existed in the functions of SA-CD19-CAR T cells and CD19-CAR T cells.

#### [<sup>68</sup>Ga]Ga-DOTA-biotin PET imaging in a solid tumor model

Representative coronal MicroPET images of mice bearing CD19<sup>+</sup> K562 tumor treated with CAR T cells after injection of [<sup>68</sup>Ga]Ga-DOTA-biotin are shown in Fig. 2A. Radioactivities were observed to be more accumulated in the tumors treated with SA-CD19-CAR T cells than in counterparts with CD19-CAR T cells. ROI analysis revealed that the uptakes in the CD19<sup>+</sup> K562 tumors were  $0.67 \pm 0.32$  ID%/g and  $1.26 \pm 0.13$  ID%/g at 30 min and 96 h p.i. after injection of SA-CD19-CAR T cells respectively. On the contrary, the corresponding values were  $0.18 \pm 0.05$  ID%/g at 96 h after injection of CD19-CAR T cells (Fig. 2B). Besides, radioactivities were also observed in lungs, livers, spleens, and the uptake values were determined to be  $0.71 \pm 0.13$ ,  $1.25 \pm 0.15$ ,  $0.76 \pm 0.15$  ID%/g respectively at 96 h p.i. in the

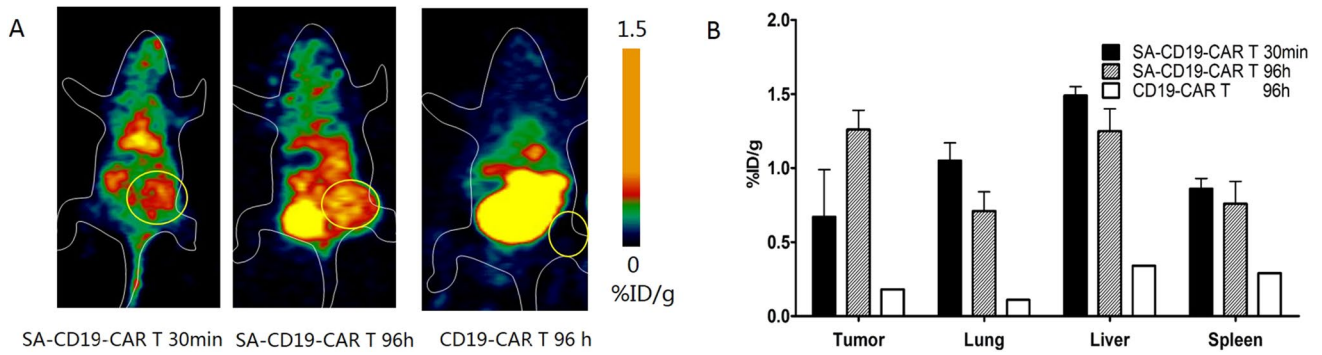


**Fig. 2** [<sup>68</sup> Ga]Ga-DOTA-biotin PET imaging in CD19<sup>+</sup> K562 solid tumor. **A** Decay-corrected whole-body PET images of mice-bearing CD19<sup>+</sup> K562 tumors infused with CAR T cells after injection of

[<sup>68</sup> Ga]Ga-DOTA-biotin. Cycles indicate the location of tumors. **B** Quantification of radioactivities in CD19<sup>+</sup> K562 xenografts models infused with SA-CD19-CAR T cells

mice after administration with SA-CD19-CAR T cells. At the same time points, the uptakes of lungs, liver, and spleen in mice treated with CD19-CAR T cells were  $0.11 \pm 0.03$ ,  $0.34 \pm 0.01$ , and  $0.29 \pm 0.03$  ID%/g respectively.

**Pharmacodynamics and pharmacokinetics study in whole-body hematologic neoplasms**

CD19-expressing Raji human B cell leukemia animal model was confirmed to be efficiently cured by CAR T cells. Thus, the model was selected for determining the pharmacodynamics (PD) of CD19-CAR T cells by bioluminescence imaging and simultaneously evaluating the pharmacokinetics (PK) of the cells using [<sup>68</sup> Ga] Ga-DOTA-biotin PET imaging. By day 0, bioluminescence

imaging indicated that numerous tumor cells were found in all mice (Fig. 3). Compared with the control group, the tumor burdens were significantly reduced in the mice infused with CAR T cells by day 6 and day 9 respectively. On day 6, the fluorescence intensity was determined to be  $22.09 \pm 11.52 \times 10^6$ ,  $27.04 \pm 5.25 \times 10^6$ , and  $58.16 \pm 14.79 \times 10^6$  in mice treated with SA-CD19-CAR T cells, CD19-CAR T cells, and medium respectively. On day 9, The fluorescence intensity was determined to be  $15.79 \pm 1.96 \times 10^6$ ,  $16.06 \pm 1.21 \times 10^6$ ,  $129.38 \pm 11.53 \times 10^6$  in mice treated with SA-CD19-CAR T cells, CD19-CAR T cells, and medium respectively. At 15 days after treatment with CAR T cells, none of the fluorescence intensity was detected. On the contrary, no mice in control groups treated with medium survived.

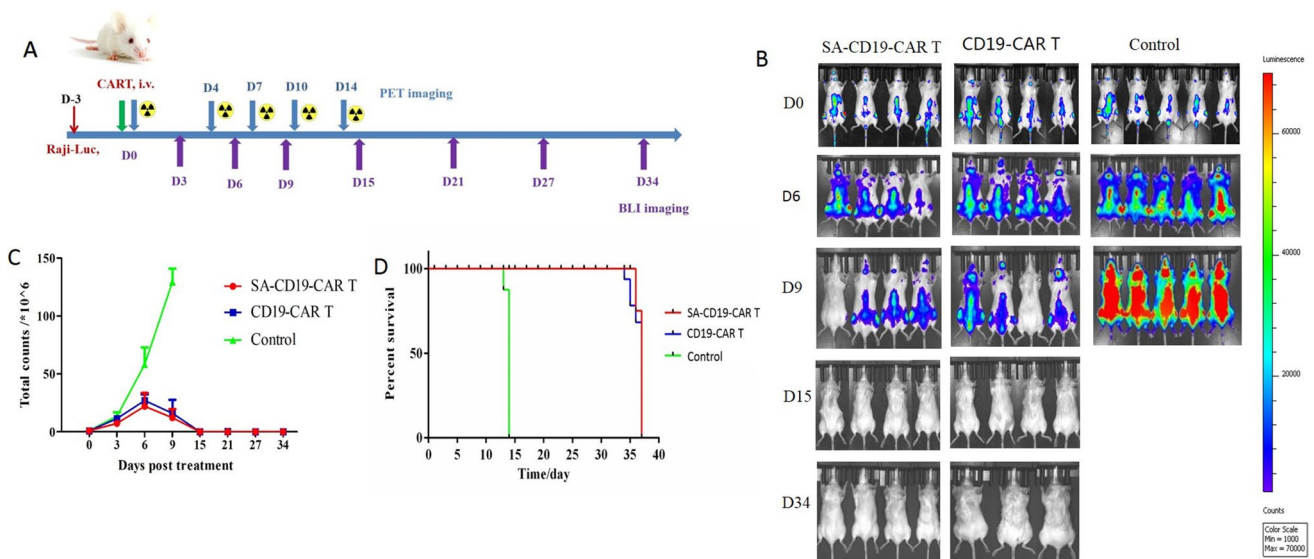


**Fig. 3** **A** Schemes of bioluminescence and survival analysis of NCG mice engrafted with Raji human Burkitt’s lymphoma expressing CD19 treated with CAR T cells; **B** representative bioluminescent

images of each treatment group; **C** mean luminescence of quantified tumor growth for each treatment group; **D** survival curves of mice in each group

Low levels of radioactivity were detected from microPET images of all mice at day 7 after treatment (Fig. 4). Quantitative analysis revealed that the lung, liver, spleen, and kidney uptake of [ $^{68}\text{Ga}$ ]Ga-DOTA-biotin in mice-bearing tumors after treatment with CD19-CAR T cells and SA-CD19-CAR T cells were  $0.03 \pm 0.01$ ,  $0.18 \pm 0.03$ ,  $0.08 \pm 0.01$ ,  $0.43 \pm 0.02$  ID%/g and  $0.04 \pm 0.01$ ,  $0.21 \pm 0.03$ ,  $0.12 \pm 0.02$ ,  $0.49 \pm 0.13$  ID%/g respectively. At the same time points, the corresponding values were  $0.03 \pm 0.01$ ,  $0.17 \pm 0.02$ ,  $0.12 \pm 0.03$ , and  $0.42 \pm 0.04$  ID%/g in mice of the control group respectively.

## Discussion

CAR T cell therapy is an encouraging approach for decreasing tumor progression and extending patient survival. The therapy efficacy is significantly close to the proliferation profiles of CAR T cells. Currently, real-time monitoring of the behaviors of the cells in the body through qPCR or flow cytometry remains a challenge. Accurate information about behaviors of CAR T cells from PET imaging using a reporter gene system will be helpful to precise and effective therapy.

In our previous study, [ $^{68}\text{Ga}$ ]Ga-labeled biotin was successfully synthesized [22]. It showed that the concentrations of SA could be quantitatively determined by  $^{68}\text{Ga}$ -DOTA-biotin using both in vitro radio-TLC and in vivo PET

imaging after stereotactic injection. Further PET imaging revealed that the levels of SA expressed in SA-CD19-CAR T cells could be accurately measured by the tracer. Thus, [ $^{68}\text{Ga}$ ]Ga-DOTA-biotin-SA was chosen as a reporter-probe system to track CAR T cells in living bodies.

As a viable imaging reporter, it is important that the introduction of the marker should not affect the antitumor activity of CD19-CAR T cells. It was found that the proliferation profiles of SA-CD19-CAR T cells were consistent with those of CD19-CAR T cells. Compared with the control group, the LDH cytotoxicity assay preliminarily showed that the viability of the Raji tumor cells was significantly decreased by co-incubation with naive or modified CD19-CAR T cells. Further experiments revealed that SA-CD19-CAR T or CD19-CAR T cells released numerous cytokines to attack tumor cells with the same levels. It confirmed that similar to the naive CD19-CAR T cells, the SA-CD19-CAR T cells own strong killing effects on Raji cancer cells. In summary, transduction of SA into CAR T cells did not affect the cell's functions and the resulting SA-CD19-CAR T cells could recognize the corresponding tumor antigen and destroy the tumors.

Our previous study confirmed that there existed a significant positive correlation between PD and targeting properties of CD19-CAR T cells in solid tumors [29]. However, the proliferation of CAR T cells was not observed by direct labeling with [ $^{89}\text{Zr}$ ]Zr-oxine during the period of

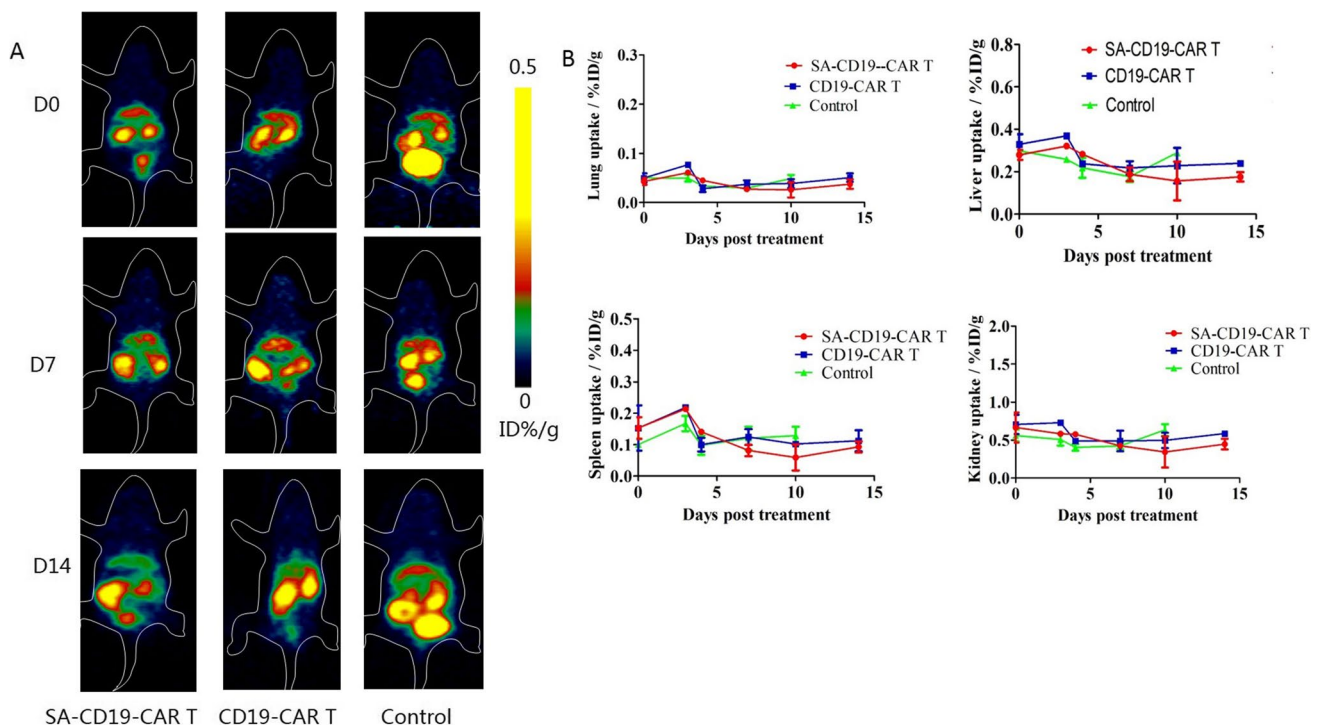


**Fig. 4** **A** Representative PET images of each treatment group on day 0, 7, and 14. **B** Quantification of radioactivities in CD19<sup>+</sup> Raji hematologic neoplasms

treatment. In vivo bioluminescence imaging showed that the tumor burden was significantly decreased after treatment with CD19-CAR T cells. It implied that the amounts of cells were enhanced in vivo since the success of CAR-T therapy was mainly dependent on the proliferation of CAR T cells. However, PET imaging with [ $^{89}\text{Zr}$ ] $^{89}\text{Zr}$ -oxine revealed that no significant difference existed in the uptakes in CD19-positive tumors (about 0.5%ID/g) from 0 to 7 days after therapy. It suggested that [ $^{89}\text{Zr}$ ] $^{89}\text{Zr}$ -oxine PET imaging might not be suitable for tracking the proliferation profiles of CAR T cells in solid tumors. Fortunately, the proliferation of CAR T cells in solid tumors could be clearly observed by [ $^{68}\text{Ga}$ ]Ga-DOTA-biotin PET imaging in this study. Accumulated radioactivity was found in solid tumors at 30 min p.i and increased nearly 1 time at 96 h p.i. Importantly, the proliferation of CAR T cells in tumors could be detected earlier than those of other reporter probes such as [ $^{18}\text{F}$ ] $^{18}\text{F}$ -DCFPyL toward PSMA (96 h vs. 5 days respectively)<sup>21</sup>. Moreover, radioactivity was also accumulated in the normal organs such as the lung, liver, and spleen, which was following the behaviors of intravenously infused CAR T cells [16, 29]. It seemed that the SA reporter approach for CAR T cell tracking by [ $^{68}\text{Ga}$ ]Ga-DOTA-biotin PET is promising to effectively monitor the behaviors of the adoptive cells.

Encouraged by the favorable outcomes in solid tumors, PK and PD of CAR T cells were further evaluated in mice-bearing whole-body hematologic tumor. Raji human Burkitt's lymphoma is the first hematopoietic human cell line and could be used as an excellent transfection host for a variety of molecular biology applications. A luciferase-expressing Raji cell line (Raji-Luc) is an excellent model to evaluate CD19-directed CAR T therapies through tracking disease progression and therapeutic response over time by in vivo optical imaging. BLI imaging confirmed that SA-CD19-CAR T cells could eliminate the tumor cells. Also, compared to the control group, the survival of mice treated with SA-CD19-CAR T cells was extended nearly 20 days, which is consistent with counterparts of the unmodified CAR T cells.

For evaluating the PK of CAR T cells, qPCR was firstly applied to determine the amounts of CAR T cells in the peripheral blood of each mouse<sup>30</sup>. However, no CAR T cells were detected during therapy. PET imaging with reporter-probes owned favorable sensitivity in visualizing CAR T cells. It was reported that the lowest numbers of CAR T cells detected by a reporter–PET imaging in mice could reach 2000 to 40,000 cells located at matrigel with tiny volumes (50  $\mu\text{L}$ ) (about  $4 \times 10^5$  to  $8 \times 10^6$  cells per ml) [19, 30]. Thus, it was hypothesized that [ $^{68}\text{Ga}$ ]Ga-DOTA-biotin PET imaging could facilitate the assessment of PD. Unfortunately, low uptakes of [ $^{68}\text{Ga}$ ]Ga-DOTA-biotin were found in the mice-bearing Raji tumors, which may be a result of low sensitivity. Compared to K562 solid tumor xenografts located in

small volumes (100–300  $\text{mm}^3$ ), Raji hematologic tumors is distributed in the whole body of mice through blood transport and the distributed volumes of Raji tumor in mice were about 200 times (based on the average of 20 g body weight) higher than those of solid tumor. It was estimated that the concentrations of CAR T cells in mice bearing Raji tumors were nearly  $2.5 \times 10^5$  cells per ml (dividing  $5 \times 10^6$  cells by 20 ml), which is close to or below the minimum detectable concentrations of CAR T cells. To our knowledge, no satisfactory images of CAR T cells in the Raji tumor model by the reporter probe were acquired. Further efforts to improve the phenomenon are undergoing.

## Conclusion

SA was successfully introduced into anti-CD19 CAR T cells with no loss of viability and antitumor function. SA-biotin pair PET imaging can specifically visualize the proliferation profiles of CAR T cells in solid tumors. However, the PK-PD effect of CAR T cells in whole-body hematologic malignancies needs further investigation.

**Funding** This work was partially supported by the Leading Technology Foundation Research Project of Jiangsu Province (BK20192005), National Natural Science Foundation (31971316, 82104318).

## Declarations

**Conflict of interest** The authors declare no competing interests.

## References

1. Reiser V. Beyond CAR. T-cell therapy: continued monitoring and management of complications. *J Adv Pract Oncol.* 2020;11:159–67.
2. Ellis GI, Sheppard NC, Riley JL. Genetic engineering of T cells for immunotherapy. *Nat Rev Genet.* 2021;22:427–47.
3. Moreno-Cortes E, Forero-Forero JV, Lengerke-Diaz PA, Castro JE. Chimeric antigen receptor T cell therapy in oncology - pipeline at a glance: analysis of the ClinicalTrials.gov database. *Crit Rev Oncol Hematol.* 2021;159:103239.
4. Labbé RP, Vessillier S, Rafiq QA. Lentiviral vectors for T cell engineering: clinical applications, bioprocessing and future perspectives. *Viruses.* 2021;13.
5. Maloney DG, Kuruvilla J, Liu FF, Kostic A, Kim Y, Bonner A, et al. Matching-adjusted indirect treatment comparison of liso-cel versus axi-cel in relapsed or refractory large B cell lymphoma. *J Hematol Oncol.* 2021;14:140.
6. Mihályová J, Hradská K, Jelínek T, Motais B, Celichowski P, Hájek R. Promising Immunotherapeutic modalities for B-cell lymphoproliferative disorders. *Int J Mol Sci.* 2021;22.
7. Ali S, Kjekken R, Niederlaender C, Markey G, Saunders TS, Opsata M, et al. The European Medicines agency review of

- Kymriah (Tisagenlecleucel) for the treatment of acute lymphoblastic leukemia and diffuse large B-cell lymphoma. *Oncologist*. 2020;25:e321–7.
8. Singh AK, McGuirk JP. CAR T cells: continuation in a revolution of immunotherapy. *Lancet Oncol*. 2020;21:e168–78.
  9. June CH, O'Connor RS, Kawalekar OU, Ghassemi S, Milone MC. CAR T cell immunotherapy for human cancer. *Science*. 2018;359:1361–5.
  10. Ghorashian S, Kramer AM, Onuoha S, Wright G, Bartram J, Richardson R, et al. Enhanced CAR T cell expansion and prolonged persistence in pediatric patients with ALL treated with a low-affinity CD19 CAR. *Nat Med*. 2019;25:1408–14.
  11. Sarikonda G, Pahuja A, Kalfoglou C, Burns K, Nguyen K, Ch'en IL, et al. Monitoring CAR T cell kinetics in clinical trials by multiparametric flow cytometry: Benefits and challenges. *Cytometry B Clin Cytom*. 2021;100:72–8.
  12. Qu C, Ping N, Kang L, Liu H, Qin S, Wu Q, et al. Radiation priming chimeric antigen receptor T-cell therapy in relapsed/refractory diffuse large B-cell lymphoma with high tumor burden. *J Immunother*. 2020;43:32–7.
  13. Yan L, Qu S, Shang J, Shi X, Kang L, Xu N, et al. Sequential CD19 and BCMA-specific CAR T-cell treatment elicits sustained remission of relapsed and/or refractory myeloma. *Cancer Med*. 2021;10:563–74.
  14. Saeed M, Xu Z, De Geest BG, Xu H, Yu H. Molecular imaging for cancer immunotherapy: seeing is believing. *Bioconjug Chem*. 2020;31:404–15.
  15. Wei W, Rosenkrans ZT, Liu J, Huang G, Luo QY, Cai W. ImmunoPET: Concept, design, and applications. *Chem Rev*. 2020;120:3787–851.
  16. Wang XY, Wang Y, Wu Q, Liu JJ, Liu Y, Pan DH, et al. Feasibility study of (68)Ga-labeled CAR T cells for in vivo tracking using micro-positron emission tomography imaging. *Acta Pharmacol Sin*. 2021;42:824–31. <https://doi.org/10.1038/s41401-020-00511-5>.
  17. Weist MR, Starr R, Aguilar B, Chea J, Miles JK, Poku E, et al. PET of adoptively transferred chimeric antigen receptor T cells with (89)Zr-oxine. *J Nucl Med*. 2018;59:1531–7.
  18. Keu KV, Witney TH, Yaghoubi S, Rosenberg J, Kurien A, Magnusson R, et al. Reporter gene imaging of targeted T cell immunotherapy in recurrent glioma. *Sci Transl Med*. 2017;9.
  19. Minn I, Huss DJ, Ahn HH, Chinn TM, Park A, Jones J, et al. Imaging CAR T cell therapy with PSMA-targeted positron emission tomography. *Sci Adv*. 2019;5:eaaw5096.
  20. Vedvyas Y, Shevlin E, Zaman M, Min IM, Amor-Coarasa A, Park S, et al. Longitudinal PET imaging demonstrates biphasic CAR T cell responses in survivors. *JCI Insight*. 2016;1:e90064.
  21. Sedlak SM, Schendel LC, Gaub HE, Bernardi RC. Streptavidin/biotin: tethering geometry defines unbinding mechanics. *Sci Adv*. 2020;6:eaay5999.
  22. Liu J, Xu N, Wang X, Wang Y, Wu Q, Li X, et al. Quantitative radio-thin-layer chromatography and positron emission tomography studies for measuring streptavidin transduced chimeric antigen receptor T cells. *J Chromatogr B Analyt Technol Biomed Life Sci*. 2021;1182:122944.
  23. Hoegger MJ, Longtine MS, Shim K, Wahl RL. Bioluminescent tumor signal is mouse strain and pelt color dependent: experience in a disseminated lymphoma model. *Mol Imaging Biol*. 2021;23:697–702.
  24. Wen H, Qu Z, Yan Y, Pu C, Wang C, Jiang H, et al. Preclinical safety evaluation of chimeric antigen receptor-modified T cells against CD19 in NSG mice. *Ann Transl Med*. 2019;7:735.
  25. Kang L, Tang X, Zhang J, Li M, Xu N, Qi W, et al. Interleukin-6 knock-down of chimeric antigen receptor-modified T cells significantly reduces IL-6 release from monocytes. *Exp Hematol Oncol*. 2020;9:11.
  26. Gu B, Shi BY, Zhang X, Zhou SY, Chu JH, Wu XJ, et al. Allogeneic haematopoietic stem cell transplantation improves outcome of adults with relapsed/refractory Philadelphia chromosome-positive acute lymphoblastic leukemia entering remission following CD19 chimeric antigen receptor T cells. *Bone Marrow Transplant*. 2021;56:91–100.
  27. Zhang Y, Li J, Lou X, Chen X, Yu Z, Kang L, et al. A prospective investigation of bispecific CD19/22 CAR T cell therapy in patients with relapsed or refractory B cell non-hodgkin lymphoma. *Front Oncol*. 2021;11:664421.
  28. Chen LY, Kang LQ, Zhou HX, Gao HQ, Zhu XF, Xu N, et al. Successful application of anti-CD19 CAR T therapy with IL-6 knocking down to patients with central nervous system B-cell acute lymphocytic leukemia. *Transl Oncol*. 2020;13:100838.
  29. Wu Q, Wang Y, Wang X, Liang N, Liu J, Pan D, et al. Pharmacokinetic and pharmacodynamic studies of CD19 CAR T cell in human leukaemic xenograft models with dual-modality imaging. *J Cell Mol Med*. 2021;25:7451–61.
  30. Sakemura R, Bansal A, Siegler EL, Hefazi M, Yang N, Khadka RH, et al. Development of a clinically relevant reporter for chimeric antigen receptor T-cell expansion, trafficking, and toxicity. *Cancer Immunol Res*. 2021;9:1035–46.

**Publisher's note** Springer Nature remains neutral with regard to jurisdictional claims in published maps and institutional affiliations.

Springer Nature or its licensor holds exclusive rights to this article under a publishing agreement with the author(s) or other rightsholder(s); author self-archiving of the accepted manuscript version of this article is solely governed by the terms of such publishing agreement and applicable law.